

Attractive energy contribution to nanoconfined fluids behavior: the normal pressure tensor

F. Heidari · T. Keshavarzi · G. A. Mansoori

Received: 29 July 2010/Accepted: 18 October 2010/Published online: 3 November 2010
© Springer-Verlag 2010

Abstract The aim of our research is to demonstrate the role of attractive intermolecular potential energy on normal pressure tensor of confined molecular fluids inside nanoslit pores of two structureless purely repulsive parallel walls in xy plane at $z = 0$ and $z = H$, in equilibrium with a bulk homogeneous fluid at the same temperature and at a uniform density. To achieve this we have derived the perturbation theory version of the normal pressure tensor of confined inhomogeneous fluids in nanoslit pores:

$$P_{ZZ} = kT\rho(Z_1) + \pi kT\rho(Z_1) \int_{-d}^0 \rho(Z_2) Z_2^2 g_{Z,H}(d) dZ_2 \\ - \frac{1}{2} \iint_0^{2\pi} \phi'(\vec{r}_2) \rho(Z_1) \rho(Z_2) g_{Z,H}(r_2) \\ \times \frac{Z_2^2}{(R_2^2 + Z_2^2)^{\frac{3}{2}}} R_2 dR_2 dZ_2 d\Theta; \quad |\vec{r}_2| > d$$

In which R , Θ , Z are the cylindrical coordinate's notations and $|\vec{r}_2| = \sqrt{R_2^2 + Z_2^2}$. Assuming the truncated-Lennard-Jones potential, the third term represents the attractive intermolecular potential energy contribution to the normal pressure tensor. We report solution of this equation for the truncated-Lennard-Jones confined fluid in nanoslit pores, and we demonstrate the role of attractive potential energy by comparing the results of Lennard-Jones and hard-sphere

fluids. Our numerical calculations show that the normal pressure tensor has an oscillatory form versus distance from the walls for all confined fluids. The oscillations increase with reduced bulk density and decrease with fluid–fluid attraction. It also becomes broad and smooth with pore width at constant temperature and density. In comparison with hard-sphere confined fluids, the values of the normal pressure for LJ fluids at all distances from the walls are less than the hard-sphere fluids. This analytic pressure tensor equation is a useful tool to understand the role of attractive and repulsive forces in the normal pressure tensor and to predict phase behavior of nanoconfined fluids.

Keywords Attractive intermolecular interaction · Density functional theory · Hard-Sphere fluid · Inhomogeneous fluid · Lennard-Jones fluid · Nanoslit pore · Nanoconfined fluid · Normal pressure tensor · Perturbation theory · Repulsive intermolecular interaction

1 Introduction

Nanoconfined fluids behavior, especially the density and pressure tensor, depends on spatial direction and position where the measurement is made, and it is not the same as the macroscopic (bulk) fluid behavior. It is now known that molecular fluids in nanotubes and in nanoslit pores at equilibrium are inhomogeneous and anisotropic due to nanoconfinement and wall effects. The oscillatory behavior near a wall in general has been investigated with different methods by various investigators in the past (Zhou 2000; Yu and Wu 2002; Dong et al. 2005; Ziarani and Mohamad 2006; Eijkel and Berg 2006; Keshavarzi et al. 2006, 2010). Recently Keshavarzi et al. (2010) reported derivation of the general equation for the normal pressure tensor of the

F. Heidari · T. Keshavarzi
Department of Chemistry, Isfahan University of Technology,
Isfahan, Iran

G. A. Mansoori (✉)
Department of BioEngineering, University of Illinois at Chicago,
M/C 063, Chicago, IL 60607-7052, USA
e-mail: mansoori@uic.edu

confined fluids in nanoslit pores. The resulting equation was then applied for a hard-sphere fluid confined in nanoslit pores to predict its normal pressure tensor profile. A hard-sphere fluid model even though can represent the essential configurational features of real fluids, it lacks the attractive part of the intermolecular potential energy function.

We report here our formulation for the analytic solution of prediction of the behavior of real confined fluid in nanosystems. As an example we use the truncated-Lennard-Jones fluid in the calculations reported here. Lennard-Jones model is shown to be a realistic model for simple molecular fluids in macroscopic systems and we assume to be equally valid for confined fluids in nanoslit pores. The theoretical basis of our approach is the statistical mechanical perturbation theory of fluids already developed and shown to be quite successful in predicting the behavior of macroscopic fluid systems (Mansoori et al. 1969; Lan and Mansoori 1975; Barker and Henderson 1976; Kang et al. 1985; Zhou 2006).

Like Keshavarzi et al. (2010) (from now on it is referred to as “Paper 1”), we consider a fluid confined in a nanoslit pore consisting of two structureless and parallel walls in the $X-Y$ plane of $X-Y-Z$ rectangular coordinate system located at $Z = 0$ and $Z = H$, i.e., separated by length H in the Z direction as shown in Fig. 1 of Paper 1. This means the Z direction is perpendicular to the wall.

We also assume the confined fluid in the nanoslit pore is in equilibrium with a bulk fluid at the same temperature and chemical potential. It is clear that fluid in such a nanoslit pore is inhomogeneous, and therefore, all of its thermodynamic properties are functions of the local density. The local density is a function of the width of nanoslit “ H ”, bulk density “ $\rho_{\text{MAC. BULK}}$ ”, absolute temperature “ T ”, and the interaction of fluid–fluid and the fluid–wall molecules. In Paper 1 using statistical mechanics of small/nano systems, the general equation for the normal pressure tensor was derived which is applicable for all confined fluids in nanoslits with all kinds of wall–fluid and fluid–fluid interaction as:

$$P_{ZZ}(r_{1Z}) = kT\rho(r_{1Z}) + \rho(r_{1Z})\frac{\partial\phi_{\text{ext}}}{\partial r_{1Z}}dr_{1Z} - \frac{1}{2}\int_v \phi'(\vec{r}_{12})\rho^{(2)}(\vec{r}_{12}, \vec{r}_1)\frac{(r_{12Z})^2}{|\vec{r}_{12}|}d\vec{r}_{12} \quad (1)$$

where $\vec{r}_{12} \equiv \vec{r}_1 - \vec{r}_2$ is the intermolecular position vector of molecule 2 with respect to molecule 1 and $r_{12Z} = |\vec{r}_{12}|_Z$ is the projection of distance of molecule 1 from molecule 2 in the Z direction, r_{1Z} is the projection of the distance of molecule 1 from the wall on the Z -coordinate, $\phi(\vec{r}_{12})$ is the intermolecular pair-potential energy function, and ϕ_{ext} is the molecules–wall interaction potential function. For the

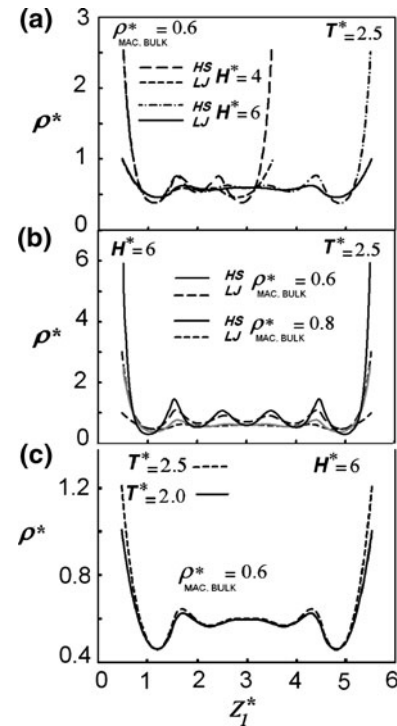


Fig. 1 **a** comparison of local density of LJ and HS confined fluid in nanoslit pores with hard walls versus Z_1 at $\rho^* = 0.6$ and $T^* = 2.5$ for two different pore widths equal to 4 and 6. **b** Same as **a** except at $H^* = 6$ for two different reduced densities equal to 0.6 and 0.8. **c** Same as **b** except at $\rho^* = 0.6$ for two different reduced temperatures equal to 2 and 2.5

nanoslit pore we can clearly assume $\rho(r_{1Z}) = \rho(Z_1)$ which is the local density of the molecule 1. The term $\rho^{(2)}(\vec{r}_{12}, \vec{r}_1)$ is the pair-probability density distribution and P_{ZZ} is the normal pressure tensor. The first term in the right-hand side of Eq. 1 is the kinetic contribution, the second term is the wall–fluid interaction contribution, and the third term is intermolecular interaction contribution.

For the general solution of Eq. 1 for normal pressure tensor we need the expression for the radial distribution function of the confined fluid and its density profile data. We currently do not have the expression for the radial distribution function of confined fluid, but through the use of the density functional theory (DFT) we can readily produce the density profile data as a function of the density of a macroscopic bulk fluid “ $\rho_{\text{MAC. BULK}}$ ”, in equilibrium with the fluid inside the nanoslit pore. To bypass the need for the radial distribution function we have inevitably used the perturbation theory. In what follows we obtain the equation for the normal pressure tensor of a confined real fluid in nanoslit pores based on the perturbation theory. Then, as a practical example we apply the resulting theory for a Lennard-Jones nanoconfined fluid system.

2 The theory

For investigation on the role of attractive intermolecular forces on normal pressure tensor of fluids confined in a nanoslit pore with structureless hard walls we assume the system consists of N real molecules with the hard-core (hc) diameter d confined between two parallel hard walls with macroscopic areas and with pore width equal to H .

Based on the statistical mechanical perturbation and variational theories, the pair-intermolecular potential energy may be separated in two parts (Mansoori et al. 1969; Lan and Mansoori 1975; Barker and Henderson 1976; Kang et al. 1985; Zhou 2006):

$$\phi = \phi_{\text{reference}} + \phi_{\text{perturbed}} \quad (2)$$

where $\phi_{\text{reference}}$ is the intermolecular potential energy of the reference system and $\phi_{\text{perturbed}}$ is the contribution of perturbation (attractive) part. Such separation in configuration potential energy also separates these contributions in the pair-potential energy.

For macroscopic systems there exist a variety of methods to perform perturbation or variational calculations to choose the reference potential energy function and its parameters (Mansoori et al. 1969; Lan and Mansoori 1975; Barker and Henderson 1976; Kang et al. 1985; Zhou 2006). However, the validity of such methods needs to be proven for nanosystems before we can use them. In the present report we choose a special perturbation method which is valid for, both, nano- and macro-systems. This choice enables us to clearly estimate the attractive intermolecular force contribution to the normal pressure tensor of confined fluids in nanoslit pores.

In our perturbation approach we perturb a realistic intermolecular potential energy function around the hard-sphere (reference) potential energy function, called hard-core (hc) as follows,

$$\phi_{\text{reference}} = \phi_{(\text{hc})}(r_{12}) \begin{cases} = 0 & \text{for } |\vec{r}_2 - \vec{r}_1| > d \\ = \infty & \text{for } |\vec{r}_2 - \vec{r}_1| \leq d \end{cases}, \quad (3)$$

$$\phi_{(\text{perturbed})} = \begin{cases} = \phi(\vec{r}_{12}) & \text{for } |\vec{r}_2 - \vec{r}_1| > d \\ = 0 & \text{for } |\vec{r}_2 - \vec{r}_1| \leq d \end{cases}, \quad (4)$$

where in general,

$$\phi(\vec{r}_{12}) = f(r_{12}; \text{molecular angles, polarities, electrostatics, etc.}), \quad (5)$$

and d is the hard-core diameter.

Like in Paper 1, the external potential, φ_{ext} , which is imposed by walls on the confined fluid is assumed to be of purely repulsive nature as follows:

$$\varphi_{(\text{hc})}^{\text{Ext}}(r_{1Z}) \begin{cases} 0 & \text{for } \frac{d}{2} < r_{1Z} < H - \frac{d}{2} \\ \infty & \text{for } H - \frac{d}{2} \leq r_{1Z} \leq \frac{d}{2} \end{cases}. \quad (6)$$

In this equation r_{1Z} is the projection of the distance of molecule 1 from the wall on the Z direction. In perturbation theory with analogy to potential energy the other thermodynamic properties may be separated into two parts. For example (Mansoori et al. 1969) for pressure of the system we have:

$$P_{ZZ} = P_{ZZ}^{(\text{hc})} + P_{ZZ}^{(\text{perturbed})} \quad (7)$$

where $P_{ZZ}^{(\text{hc})}$ is the local normal pressure of unperturbed (reference) hard-core system and $P_{ZZ}^{(\text{perturbed})}$ is the contribution of perturbation (attractive) part.

Since the local density is uniform in x and y directions (it is a function of Z beside T , H , and $\rho_{\text{MAC_BULK}}$ (the density of a macroscopic bulk fluid system in equilibrium with the fluid inside the nanoslit pore)). Since the nanoslit width is limited in the Z direction we write Eq. 1 in the cylindrical coordinates in which the variable Z will appear explicitly. We then use the cylindrical coordinate's notations (R , Θ , Z), where R refers to the radial coordinate and Θ is the azimuthal coordinate. Now since $|\vec{r}_{12}| = r_{12} = \sqrt{R_{12}^2 + Z_{12}^2}$ and considering Eqs. 4 and 6 in the cylindrical coordinates, Eq. 1 will assume the following form

$$P_{ZZ}(Z_1) = \rho(Z_1)kT - \frac{1}{2} \iiint \phi'(\vec{r}_{12})\rho^{(2)}(r_{12}, r_1) \times \frac{Z_{12}^2}{(R_{12}^2 + Z_{12}^2)^{\frac{1}{2}}} R_{12} dR_{12} dZ_{12} d\Theta. \quad (8)$$

In deriving Eq. 8 from Eq. 1 the second term of Eq. 1 vanishes because according to Eq. 6 the wall-fluid interaction term for nanoslit pore with two hard walls is zero. We now use the definition of $\rho^{(2)}$ with respect to the RDF (radial distribution function) $g_{Z,H}(r_{12})$ according to the “local-density approximation” which is valid for weakly inhomogeneous systems (Kalikmanov 2001),

$$\rho^{(2)}(r_{12}, r_1) = \rho(Z_1)\rho(Z_2)g_{Z,H}(r_{12}). \quad (9)$$

The subscripts Z and H in $g_{Z,H}$ are to indicate that RDF is dependent on, both, H (the width of the nanoslit) and the width variable Z . By assuming the position of molecule “1” fixed on the coordinate center we can replace Z_{12} , r_{12} , and R_{12} with Z_2 , r_2 , and R_2 , respectively, and we can write Eq. 8 in the following form:

$$P_{ZZ}(Z_1) = \rho(Z_1)kT - \frac{1}{2} \iiint \phi'(\vec{r}_2)\rho(Z_1)\rho(Z_2)g_{Z,H}(r_2) \times \frac{Z_2^2}{(R_2^2 + Z_2^2)^{\frac{1}{2}}} R_2 dR_2 dZ_2 d\Theta, \quad (10)$$

where $r_2 = \sqrt{R_2^2 + Z_2^2}$. Now we separate the integral of Eq. 10 into two parts, $P_{ZZ}^{(\text{reference})}$ (the reference part) and $P_{ZZ}^{(\text{perturbed})}$ (the perturbed term) according to Eq. 7.

The reference part of Eq. 6 will be as follows:

$$P_{ZZ}^{(\text{reference})} = \rho(Z_1)kT - \pi\rho(Z_1) \iint \phi'_{(\text{hc})}(r_2)\rho(Z_2)g_{Z,H}(r_2) \\ \times \frac{Z_2^2}{(R_2^2 + Z_2^2)^{0.5}} R_2 dR_2 dZ_2 \quad (11)$$

Since the reference hard-core potential, $\phi'_{(\text{hc})}(r_2)$, is zero everywhere except at $(R_2^2 + Z_2^2)^{0.5} = d$ we write it in the following form:

$$\phi'_{(\text{hc})}(r_2) = -kT\delta([R_2^2 + Z_2^2]^{0.5} - d) \\ \times \exp\left(\frac{\phi_{(\text{hc})}[(R_2^2 + Z_2^2)^{0.5}]}{kT}\right), \quad (12)$$

where $\delta([R_2^2 + Z_2^2]^{0.5} - d)$ is the Dirac delta-function. By inserting Eq. 12 into Eq. 11 we get:

$$P_{ZZ}^{(\text{reference})} = \rho(Z_1)kT + \pi kT\rho(Z_1) \left[\int_{-d}^0 \rho(Z_2) \frac{Z_2^2}{(R_2^2 + Z_2^2)^{0.5}} g_{Z,H}(r_2) dZ_2 \right. \\ \left. \times \int_0^\infty \delta((R_2^2 + Z_2^2)^{0.5} - d) \exp\left(\frac{\phi_{(\text{hc})}[(R_2^2 + Z_2^2)^{0.5}]}{kT}\right) R_2 dR_2 \right] \quad (13)$$

The second integral in Eq. 13 is a Dirac integral and it has a non-zero value only when $[R_2^2 + Z_2^2]^{0.5} = d$. Therefore, Eq. 13 will simplify to the following form

$$P_{ZZ}^{(\text{reference})} = \rho(Z_1)kT + \pi kT\rho(Z_1) \int_{-d}^0 \rho(Z_2) Z_2^2 g_{Z,H}(d) dZ_2, \quad (14)$$

where $\rho(Z_1)$ and $\rho(Z_2)$ are the local densities of the real fluid in the nanoslit, $g_{Z,H}(d)$ is the RDF at the contact point, which is angle-independent, and Z_1 and Z_2 are position of molecules 1 and 2 in the Z direction, respectively. Eq. 14 is the same as Eq. 34 of Paper 1 if we replace $g_{Z,H}$ with g_{hs} ($d^{0.5}$ appearing in the 2nd term in right-hand side of Eq. 34 of Paper 1 is a type error).

To get the perturbation term of the integral in the right-hand side of Eq. 10 again we select the position of molecule “1” as the coordinate center. Therefore, Z_{12} , R_{12} and r_{12} are replaced with Z_2 , R_2 and r_2 , respectively. Also we should choose the values of Z_2 , R_2 as they generate $[r_2 = \sqrt{R_2^2 + Z_2^2} > d]$ by considering the limitation (H) in the Z direction,

$$P_{ZZ}^{\text{Perturbed}}(Z_1) = -\frac{1}{2} \iint \int_0^{2\pi} \phi'(\vec{r}_2)\rho(Z_1)\rho(Z_2)g_{Z,H}(r_2) \\ \times \frac{Z_2^2}{(R_2^2 + Z_2^2)^{1/2}} R_2 dR_2 dZ_2 d\Theta; \quad r_2 > d \quad (15)$$

Finally, by joining Eqs. 15 and 16 the equation for the normal pressure tensor of the confined fluid in nanoslit pores is derived:

$$P_{ZZ} = P_{ZZ}^{(\text{reference})} + P_{ZZ}^{(\text{perturbed})} \\ = kT\rho(Z_1) + \pi kT\rho(Z_1) \int_{-d}^0 \rho(Z_2) Z_2^2 g_{Z,H}(d) dZ_2 \\ - \frac{1}{2} \iint \int_0^{2\pi} \phi'(\vec{r}_2)\rho(Z_1)\rho(Z_2)g_{Z,H}(r_2) \\ \times \frac{Z_2^2}{(R_2^2 + Z_2^2)^{1/2}} R_2 dR_2 dZ_2 d\Theta; \quad r_2 > d \quad (16)$$

Equation 16 is a general perturbation equation for the local normal pressure tensor of confined fluids in nanoslit pores as a function of the local density and temperature. With the assumption of a realistic intermolecular potential energy function, like what is derived by Zhang et al. (2007), Eq. 16 may be used to predict the normal pressure tensor of confined realistic fluids in nanoslit pores. As an example in the present study we use the Lennard-Jones intermolecular pair-potential energy function.

3 Applications for confined Lennar-Jones fluid and approximations

In the present report for calculation of the normal pressure tensor of real fluids the truncated-Lennard-Jones (LJ) intermolecular potential energy function is used,

$$\phi(\vec{r}_{12}) = \begin{cases} 4\varepsilon \left[\left(\frac{\sigma}{r_{12}}\right)^{12} - \left(\frac{\sigma}{r_{12}}\right)^6 \right] & \text{for } |\vec{r}_{12}| > \sigma \\ \infty & \text{for } |\vec{r}_{12}| \leq \sigma \end{cases}. \quad (17)$$

To remove complications related to the choice of the hard-core diameter, d , we choose that equal to the Lennard-Jones length parameter σ , i.e., ($d = \sigma$).

In order to apply Eq. 16 for normal pressure tensor calculation we need the RDF and local density profile data.

The RDF, $g_{Z,H}$, in nanoslits is different from the bulk system RDF. It is a function of local density in the nanoslit, but due to the lack of an exact functional form for $g_{Z,H}(d)$ and $g_{Z,H}(r_2)$ we replace them with their average values, i.e.,

$$g_{Z,H}(d) \cong \langle g_{Z,H}(d) \rangle, \\ g_{Z,H}(r_2) \cong \langle g_{Z,H}(r_2) \rangle. \quad (18)$$

Then Eq. 16 will assume the following form

$$\begin{aligned} P_{ZZ} &= P_{ZZ}^{(\text{reference})} + P_{ZZ}^{(\text{perturbed})} \\ &= kT\rho(Z_1) + \pi kT\rho(Z_1)\langle g_{Z,H}(d) \rangle \int_{-d}^0 \rho(Z_2)Z_2^2 dZ_2 \\ &\quad - \frac{1}{2}\langle g_{Z,H}(r_2) \rangle \iint_0^{2\pi} \phi'(\vec{r}_2)\rho(Z_1)\rho(Z_2) \\ &\quad \times \frac{Z_2^2}{(R_2^2 + Z_2^2)^{\frac{1}{2}}} R_2 dR_2 dZ_2 d\Theta; \quad r_2 < d \end{aligned} \quad (19)$$

Then due to the lack of any information about $g_{Z,H}$ we assume

$$\langle g_{Z,H}(d) \rangle \cong \langle g_{Z,H}(r_2) \rangle \cong 1. \quad (20)$$

Then we end up with the following approximate, but manageable, expression

$$\begin{aligned} P_{ZZ} &= P_{ZZ}^{(\text{reference})} + P_{ZZ}^{(\text{perturbed})} \\ &= kT\rho(Z_1) + \pi kT\rho(Z_1) \int_{-d}^0 \rho(Z_2)Z_2^2 dZ_2 \\ &\quad - \frac{1}{2} \iint_0^{2\pi} \phi'(\vec{r}_2)\rho(Z_1)\rho(Z_2) \\ &\quad \times \frac{Z_2^2}{(R_2^2 + Z_2^2)^{\frac{1}{2}}} R_2 dR_2 dZ_2 d\Theta; \quad r_2 > d \end{aligned} \quad (21)$$

Equation 21 may be applied for prediction of the normal pressure tensor of fluids in gases and liquids states, although all the reported data in this manuscript are for the bulk fluid gaseous state. To obtain the normal pressure tensor using the above equation the local density profile for the LJ confined fluid in nanoslit pore with hard walls is necessary. The local density is a function of the pore width H , temperature T and $\rho_{\text{MAC. BULK}}$, the density of a macroscopic bulk fluid system in equilibrium with the fluid inside the nanoslit pore, called “bulk density” for short. To produce such data we used the density functional theory (Heidari et al. 2010) for an inhomogeneous fluid system. The data which we have obtained by DFT are summarized in Figure (1a–c).

Figure 1a shows the local density of the truncated LJ confined fluid in the nanoslit pore with hard walls at the reduced temperature $T^* = kT/\varepsilon = 2.5$, reduced “bulk density” $\rho_{\text{MAC. BULK}}^* = \sigma^3 \rho_{\text{MAC. BULK}} = 0.6$ and for two different reduced pore widths $H^* = H/\sigma = 4$ and 6. According to Fig. 1a the local density has an oscillatory behavior indicating layering configuration similar to the confined hard-sphere fluid behavior in nanoslits (Kamalyan et al. 2008). When the pore width increases, the number of layers increases but the height of layers decreases. The profile of the local density in Fig. 1b is the

same as in Fig. 1a but for two different reduced densities at reduced pore width $H^* = 6$ and reduced temperature $T^* = 2.5$. As it is clear from this figure by decreasing the “bulk density” the layers become more diffuse and broad. Figure (1c) shows the variation of the density profile with reduced temperature at constant H^* and $\rho_{\text{MAC. BULK}}^*$. Increasing T^* is equivalent to reducing the well depth, “ ε ”, of the potential. By decreasing the inter-particle interaction, or increasing the reduced temperature, the tendency of molecules to move into the slit becomes more and the “average density” in the pore increases.

Figure (2) shows the normal pressure tensor profile of the reference hard-sphere part of the LJ fluids (combination of 1st and 2nd terms of Eq. 21: $kT\rho(Z_1) + \pi kT\rho(Z_1) \int_{-d}^0 \rho(Z_2)Z_2^2 dZ_2$) at $\rho_{\text{MAC. BULK}}^* = 0.6$, $T^* = 2$, for two different values of $H^* = 4$ and 6. As it is shown the reference hard-sphere term has an oscillatory behavior versus reduced distance Z_1^* of the molecule 1 from the wall and the amplitude of these oscillations decreases with pore width. Also when the pore width increases, the layers of the molecule in the pore increase but the height of the layers decrease.

Figure 3a–c shows our results for attractive term of the normal pressure tensor, 3rd term of Eq. 21, for two different bulk densities, pore widths and temperatures, respectively. According to Fig. 3a at constant temperature and pore width when the “bulk density”, and as a result the average density in the nanoslit pore, increases contribution of intermolecular attractions as well as its fluctuations decrease. According to Fig. 3b at constant “bulk density” and temperature by increasing the pore width, the number of layers and their depth decrease. According to Fig. 3c by reducing the temperature the tendency of molecules to move into the nanoslit pore decreases. Therefore, their contribution to the normal pressure tensor decreases. By increasing the reduced temperature the contribution of the attractive forces on the pressure tensor as well as the depth and height of the pressure oscillations decrease.

Figure 4a shows the normal pressure tensor profile (the sum of the reference and perturbed parts) for LJ fluid

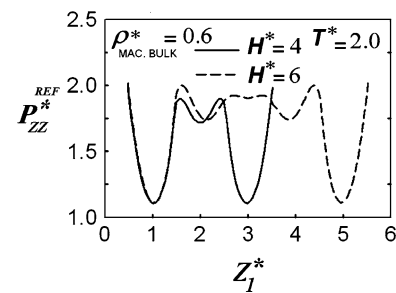


Fig. 2 The contribution of the reference part of the normal pressure tensor for LJ confined fluids in nanoslit pore with hard walls at $\rho^* = 0.6$ and $T^* = 2$ for two different pore widths $H^* = 4$ and 6

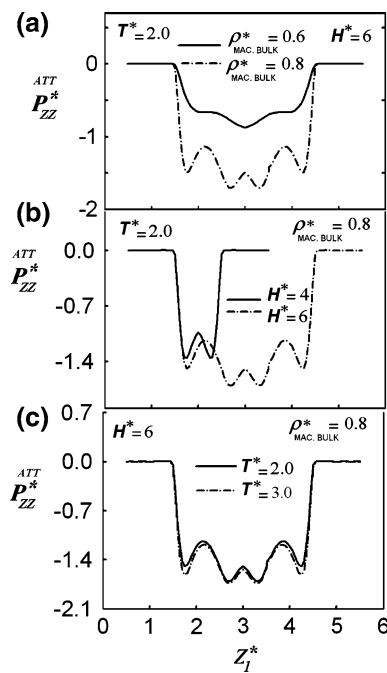


Fig. 3 **a** The contribution of the perturbed part of the normal pressure tensor for LJ confined fluids in nanoslit pore with hard walls at $H^* = 6$ and $T^* = 2$ for two different reduced densities equal to 0.6 and 0.8. **b** Same as **a** except at $\rho^* = 0.8$ for two different pore widths equal to 4 and 6. **c** Same as **b** except at $H^* = 6$ for two different reduced temperatures $T^* = 2$ and 2.5

confined in nanoslit pores at $\rho_{MAC.BULK}^* = 0.8$, $T^* = 2.5$ and 2 at $H^* = 6$. The normal pressure has a maximum value near the walls and exhibits oscillatory behavior that decreases with distance from the wall. This oscillatory behavior versus Z_1 is similar to the hard-sphere fluid normal pressure reported in Fig. 4b for the same conditions. The positions of the maxima and minima of normal pressure tensor profile occur in the half integer and integer values of Z_1 , respectively. Since the attractive force contribution of intermolecular interaction (or perturbation part) to the local pressure is negative, according to Fig. 3a–c, the normal pressure tensor of the LJ confined fluid is smaller than that of the hard-sphere confined fluid.

As we have obtained in this report and corresponding to results in Paper 1 (Keshavarzi et al. 2010), the values of the normal pressure tensor at the contact point for both hard-sphere and LJ fluids is equal to ρkT , which arises only from the kinetic contribution. This is because of our definition for normal local pressure tensor (based on the method of plain) in which only the interactions between the molecules which are between the real wall and one side of imaginary plane comes into account to calculate the normal pressure tensor. Therefore, when the imaginary plate inserts at the distance of $\sigma/2$ from the wall, at the contact point, there is not any molecule in this distance, $0 < Z_1 < \sigma/2$; therefore, there is not any contribution from the intermolecular

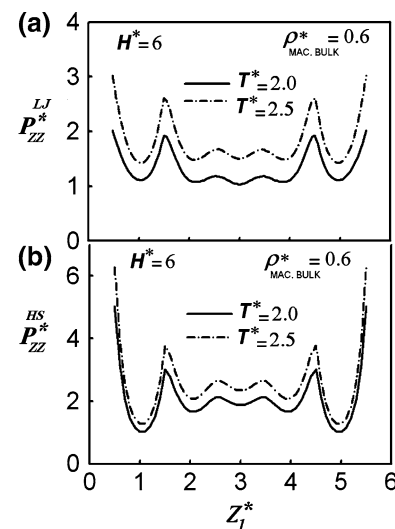


Fig. 4 The normal pressure tensor for LJ confined fluids in nanoslit pore with hard walls at $\rho^* = 0.6$ and $H^* = 6$ for two different reduced temperatures $T^* = 2$ and 2.5. **b** Same as **a** except for HS confined fluids in nanoslit pore with hard walls

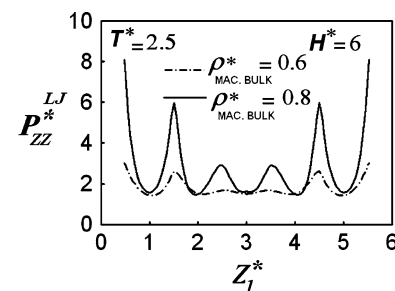


Fig. 5 The normal pressure tensor for LJ confined fluids in nanoslit pore with hard walls versus Z_1 at $H^* = 6$ and $T^* = 2.5$ for two different reduced densities $\rho^* = 0.6$ and 0.8

interaction in the pressure and so only the kinetic contribution $\rho(Z)kT$ determines the values of the normal pressure tensor at the contact point.

In Fig. 5 we report the normal pressure of the LJ fluid confined in nanoslit pore at two different reduced bulk densities of $\rho_{MAC.BULK}^* = 0.6$ and 0.8. According to this figure the height and depth of the pressure oscillations is reduced as the density is decreased.

In Fig. 6 we report the normal pressure tensor for the LJ confined fluid in nanoslit pore at $\rho_{MAC.BULK}^* = 0.6$ and $T^* = 2.5$ for two different reduced pore widths $H^* = 4$ and 6. According to Fig. 6 the number of oscillations of normal pressure tensor increases with increasing H^* .

In Fig. 7a, b we report the normal pressure tensor of the hard-sphere fluid (with molecular diameter equal to the LJ length parameter σ) and the LJ confined fluids in nanoslit for a $H^* = 6$, $T^* = 2.5$ and $\rho_{MAC.BULK}^* = 0.8$. As it is clear from this figure the normal pressure for both of two examined fluids has symmetrical oscillatory behavior

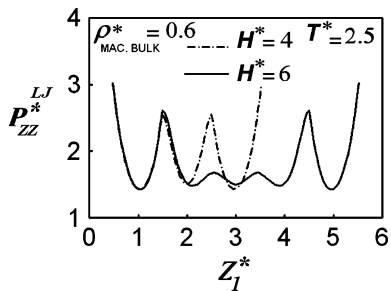


Fig. 6 The normal pressure tensor for LJ confined fluids in nanoslit pore with hard walls versus Z_1 at $\rho^* = 0.6$ and $T^* = 2.5$ for two different pore widths $H^* = 4$ and 6

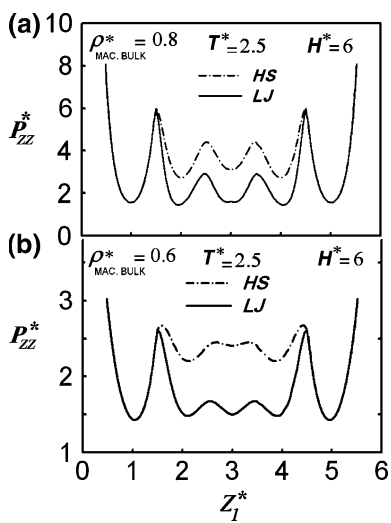


Fig. 7 **a** Comparison of normal pressure of LJ confined fluid in nanoslit with hard-core fluid at $H^* = 6$, $T^* = 2.5$ and bulk density $\rho^* = 0.8$. **b** Same as **a** except at bulk density $\rho^* = 0.6$

versus Z_1 which they decrease exponentially from the wall. Also the normal pressure tensor of LJ confined fluids for all values of Z_1 , because of the attraction term, is lower than corresponding values for hard-sphere fluids except for distances up to 1.5σ from the walls. It is because of our definition in model in which the attraction term comes into account for molecules when they are in distances more than σ , and one cannot find any molecules for distances lower than $\sigma/2$ from the walls.

Figure 7b is similar to Fig. 7a but for $\rho_{\text{MAC.BULK}}^* = 0.6$. As this figure shows when the bulk density decreases the normal pressure tensor for both fluids decreases, the layers become broader and smooth and the differences between the two pressures increase.

4 Discussion and conclusions

We have derived a general perturbation equation for predicated the normal pressure tensor of realistic

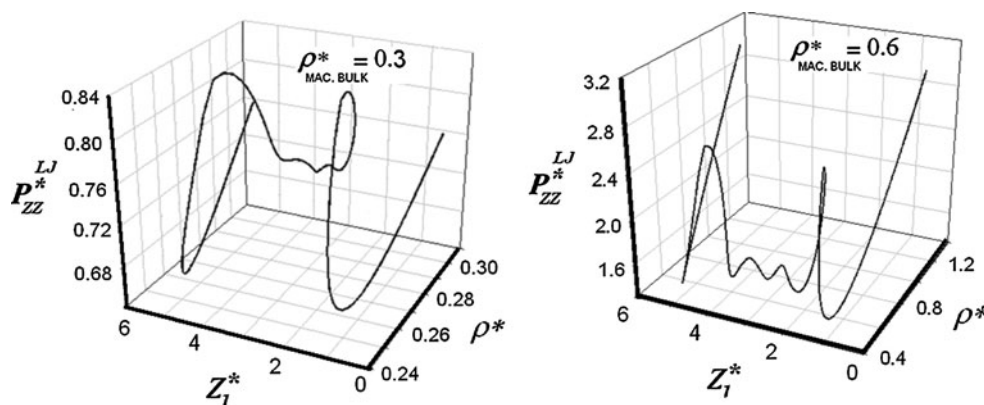
molecular fluids having both attractive and repulsive intermolecular energies. We have predicted the effect of attractive intermolecular forces on the behavior of confined fluids in nanoslit pores using the general equation for the normal pressure tensor applied to the Lennard-Jones fluid. Comparison of our results with those obtained for hard-sphere confined fluids (Keshavarzi et al. 2010) indicates that the local normal pressure tensors of both LJ and hard-sphere confined fluids have oscillatory behavior versus distance from the walls. This oscillatory behavior increases with temperature and bulk density and decrease with pore width for both cases. Also all the kinetic, repulsion, and attraction potential terms in the local normal pressure tensor of real confined fluids have oscillatory behavior.

It is shown that the attraction contribution of intermolecular interaction to local pressure is negative. As a result the normal pressure tensor of LJ confined fluid is lower than those of hard-sphere confined fluid. Our results show that at constant reduced bulk density and pore width, repulsive interactions increase with temperature; however, contribution of the attractive interactions on the pressure tensor decreases. Bulk density also affects both repulsive and attractive interactions. Our results show that at constant temperature and pore width when the “bulk density”, and as a result the average density in the nanoslit pore, increases, the contribution of intermolecular attractions as well as its fluctuations decreases; however, the contribution of repulsive interactions increases. Finally, at constant “bulk density” and temperature with increasing the pore width, the depth of oscillations of the local normal pressure decreases while the number of maximum and minimum in that increases. Temperature affects both repulsive and attractive contributions to pressure tensor. When the bulk density decreases the layers become more diffuse and broad. Therefore, the pressure between the walls decreases but maintains its oscillatory behavior. The number of layers in the pore increases with increasing pore width but their height decreases.

It is clear that while the repulsive energies predict the trend of the behavior of normal pressure tensor correctly, the attractive part of the intermolecular interactions plays a significant role in value of the confined fluids normal pressure tensor (Mansoori 2005).

Although density oscillations in the nanoslit pore is a major factor, which influences all the structural properties of confined fluids such as oscillatory behavior of normal pressure, it is not the only effective parameter. According to Eq. 16, there is no direct relation between local normal pressure and local density except for the contribution of the kinetic term, $kT\rho(Z_1)$, which is the limit of normal pressure as $\rho \rightarrow 0$. In order to demonstrate how the normal pressure and density are related we report Fig. 8. According to Fig. 8 density is not the only variable for normal pressure.

Fig. 8 Variations of the dimensionless local normal pressure and local density of the LJ nanoconfined fluid versus Z_1^* for $H^* = 6$, $T^* = 2.5$ and the bulk densities of $\rho^* = 0.3, 0.6$



We have reported all the state variables (pressure temperature and density) in dimensionless forms. Our theory is applicable for all confined molecular fluids in nanoslits. Our dimensionless computational results are applicable for all the molecular fluids for which the LJ potential function is valid, the nanoslit walls are hard-repulsive and the nanoslit is in equilibrium with a stationary bulk system. However, it is customary to quote argon as the choice fluid for which LJ potential is accurately valid.

We have demonstrated that the structure of a fluid in nanoslit pore is a function of the pore size, H , in addition to density, temperature, and intermolecular interactions between fluid molecules and walls–fluid. In the limit when the pore size, H , goes to infinity the structure of fluid becomes the same as its structure near a flat wall.

References

- Barker JA, Henderson D (1976) What is “liquid”? Understanding the states of matter. *Rev Mod Phys* 48(4):587–671
- Dong W, Chen XS, Zheng WM (2005) Thermodynamic pressure of a fluid confined in a random porous medium. *Phys Rev C* 72(1):012201
- Eijkel JC, Berg AV (2006) Nanofluidics: what is it and what can we expect from it? *Microfluid Nanofluidics* 2(1):12–20
- Heidari F, Keshavarzi T and Mansoori GA (2010) DFT simulation of the behavior of Lennard-Jones fluid in nanoslit pore (to be published)
- Kalikmanov VI (2001) Statistical physics of fluid: basic concepts and applications. Springer, Berlin
- Kamalvand M, Keshavarzi E, Mansoori GA (2008) Behavior of the confined hard-sphere fluid within nanoslits: a fundamental-measure density functional theory study. *J Nanosci* 7(4&5): 245–253
- Kang HS, Lee CS, Ree T, Ree FH (1985) A perturbation theory of classical equilibrium fluids. *J Chem Phys* 82:414. doi:[10.1063/1.448762](https://doi.org/10.1063/1.448762)
- Keshavarzi T, Sohrabi R, Mansoori GA (2006) An analytic model for nano confined fluids phase-transition: applications for confined fluids in nanotube and nanoslit. *J Comput Theor Nanosci* 3(1):134–141
- Keshavarzi T, Sedaghat F, Mansoori GA (2010) Behavior of confined fluids in nanoslit pores: the normal pressure tensor. *Microfluid Nanofluidics* 8:97–104
- Lan SS, Mansoori GA (1975) Perturbation equation of state of pure fluids. *Int J Eng Sci* 14:307–317
- Mansoori GA (2005) Principles of nanotechnology: molecular-based study of condensed matter in small systems. World Science, Publication Co., Hackensack
- Mansoori GA, Provine JA, Canfield FB (1969) Note on the perturbation equation of state of Barker and Henderson. *J Chem Phys* 41(12):5295–5299
- Yu W, Wu J (2002) Structures of hard-sphere fluids from a modified fundamental-measure theory. *J Chem Phys* 117(22): 10156–10164
- Zhang GP et al (2007) First-principles simulation of the interaction between adamantane and an atomic-force-microscope tip. *Phys Rev B* 75:035413
- Zhou S (2000) Inhomogeneous mixture system: a density functional formalism based on the universality of the free energy density functional. *J Chem Phys* 113(19):8718–8723
- Zhou S (2006) Thermodynamic perturbation theory in fluid statistical mechanics. *Phys Rev E* 74(3):031119
- Ziarani AS, Mohamad AA (2006) A molecular dynamics study of perturbed Poiseuille flow in a nanochannel. *Microfluid Nanofluidics* 2(1):12–20